Functional Micelles. 8. Micellar Catalysis of the Hydrolysis of Substituted Phenyl Carboxylates by Imidazole Containing Cationic Surfactants

Waichiro Tagaki,* Daikichi Fukushima, Toshio Eiki, and Yumihiko Yano

Contribution from the Department of Chemistry, Faculty of Engineering, Gunma University, Kiryu, Gunma, Japan

Received September 12, 1978

Micellar catalysis of dimethyl[2-(4-imidazolyl)ethyl]octadecylammonium chloride (**2**) and dimethyl[(4-imidazolyl)methyl]octadecylammonium chloride (**1a**) has been investigated for the hydrolysis of substituted phenyl esters of carboxylic acids (**5**). The catalysis was observed to occur through the rapid formation and decomposition of the acylimidazole intermediate for both neutral and anionic forms of **2** and **1a** (pH 7–9). Observed Michaelis–Menten type kinetics for the acylation step were analyzed to obtain catalytic rate constants (k_m) and the apparent association constants (K_{app}/N) separately. The effect of acyl chain length and the substituent effects on the leaving phenoxy group were then examined with respect to the k_m and K_{app}/N values. Qualitatively, the K_{app}/N values appear to be accounted for in terms of a hydrophobic binding force between the substrate and micelle. However, a case has been observed which suggests a more complex binding process involving multistep equilibria than explained simply by such hydrophobic force. For the k_m values, a linear relationship was found between log k_m and σ_p^- constants, which suggests a stabilization of transition state due to an electrostatic interaction between the positive charge of the catalyst ammonium group and the negative charge of the leaving phenoxy group. The temperature effects on the micellization of **2** and on the k_m and K_{app}/N values of *p*-methyl- and *p*-nitrophenyl hexanoates were also examined. The resulting thermodynamic parameters for the binding process (K_{app}/N) were found to be widely different for both magnitude and sign with respect to the two esters.

Micellar catalysis of a synthetic surfactant as the model of enzymic catalysis has been extensively investigated for the past decade.[1] Such micelles may be classified arbitrarily as nonfunctional and functional micelles.[1d,e] An increasing number of functional micelles have been reported in recent years. Functional groups such as amino,[2] mercapto,[3] hydroxy,[4–6] imidazole ring,[4f,7–12] hydroxamate,[12a,13] etc. have been examined. In these examples, a large rate acceleration is usually observed. However, only a very few examples seem to be effective catalytic systems. Namely, in other cases, inactivation of micelle occurs due to the formation of a stable covalent intermediate between the functional group and the substrate.

In a preliminary communication,[9a] we reported that an imidazole containing cationic surfactant (**1a**) is a remarkably effective catalyst under micellar conditions for the hydrolysis of *p*-nitrophenyl carboxylates (**5**; $n = 1$, X = *p*-NO_2). The catalysis involves a facile formation and decomposition of the acylimidazole intermediate. While in the case of the mixed micelle of *N*-myristoylhistidine and CTABr (**4a**),[8a] the acylation is fast but the next deacylation step is slow. However, it was found later by Tonellato that **1b** has an extremely low pK_1 (3.5),[9c] and the dissociated imidazole anion is the active species in such a pH region as the undissociated neutral base of **4a** is active ($pK_1 = 6.2$).[8a] In this paper, we describe the detailed accounts of catalysis of **2** in the hydrolysis of **5**. As expected, **2** has a higher pK_1 value (4.5–6) and gives a sigmoid pH–rate profile, usually observed for a neutral imidazole base. Furthermore, the deacylation step in **2** is still as fast as in **1a**.

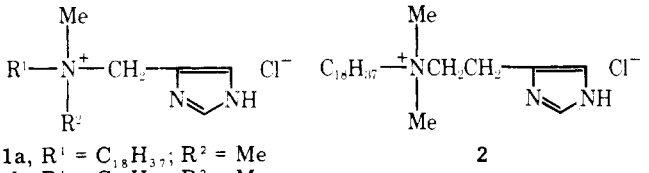

1a, $R^1 = C_{18}H_{37}$; R^2 = Me
b, $R^1 = C_{16}H_{33}$; R^2 = Me
c, $R^1 = C_{16}H_{33}$; $R^2 = CH_2CH_2OH$

2

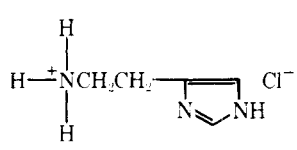

3

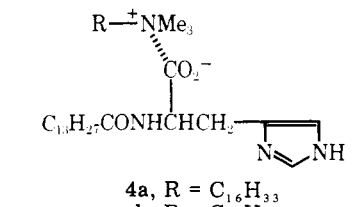

4a, R = $C_{16}H_{33}$
b, R = $C_{18}H_{37}$

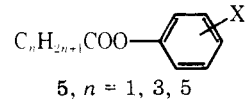

5, $n = 1, 3, 5$
X = *p*-NO_2, *p*-$COCH_3$, *m*-NO_2, *p*-Cl, H, *p*-CH_3, *m*-CH_3, *p*-*t*-Bu, *p*-CH_3O

Results and Discussion

Cmc and p*K* Values. The cmc values of **1a** and **2** determined by a dye method using eosine[14] are shown in Table I. The values for **2** were always found in a range of $3–5 \times 10^{-5}$ M under various kinetic conditions. The apparent pK_1 of **2** (4.5–6.1) measured by titration and using the modified Henderson equation [$pH = pK_{app} - \alpha \log (1 - \alpha/\alpha)$][15] was found to be concentration dependent, but it became constant at higher salt concentration (NaCl and **2**) as shown in Figure 1. Meanwhile, the kinetic pK_1 values observed in the pH–rate profile of hydrolysis (Figure 2) appear to be somewhat larger around 6.[16] The pK_1 value of **1a** was not determined. Presumably, its value is close to that of **1b** ($pK_{1(app)} = 3.5$) reported by Tonellato.[9c] The pH–rate profile (Figure 2) also suggests the pK_1 of **1a** to be low.

Kinetics. Rates vs. Surfactant Concentration. Some examples of the plots of observed pseudo-first-order rate constants against surfactant concentration are shown in Figures 3 and 4. These plots can be analyzed by assuming an ordinary kinetic scheme (eq 1) for micellar reaction[1,17] and

$$\mathrm{M} + \mathrm{S} \underset{k_o}{\overset{K_{app}}{\rightleftharpoons}} \mathrm{S\text{-}M} \xrightarrow{k_m} \mathrm{P} + \mathrm{M} \qquad (1)$$

$$k_\psi = \frac{k_o + k_m K_{app}[\mathrm{M}]}{1 + K_{app}[\mathrm{M}]} \qquad (2)$$

$$[\mathrm{M}] = \frac{C_D - \mathrm{cmc}}{N} \qquad (3)$$

$$\frac{1}{(k_\psi - k_o)} = \frac{1}{(k_m - k_o)} + \left[\frac{1}{(k_m - k_o)} \times \frac{N}{K_{app}} \times \frac{1}{(C_D - \mathrm{cmc})}\right] \qquad (4)$$

0022-3263/79/1944-0555$01.00/0

Table I. Cmc and pK Values of Surfactants

surfactant	registry no.	conditions (25 °C)	cmc, M	pK_1	pK_2
2	68437-45-6	pure water	3.25×10^{-4}	4.5–6.1[a]	13[b]
		Tris buffer (0.05 M, pH 8.07)	4.50×10^{-5}		
1a	37717-55-8	pure water	1.23×10^{-4}		
		phosphate buffer (0.05 M, pH 8.05)	1.90×10^{-5}		
1b[c]		pure water	1.05×10^{-4}	3.5	
STABr[d]	1120-02-1	pure water	4.51×10^{-4}		
		Tris buffer (0.07 M, pH 9.0)	3.02×10^{-4}		

[a] See Figure 1. [b] Reference 16b. [c] Reference 9c. [d] Octadecyltrimethylammonium bromide.

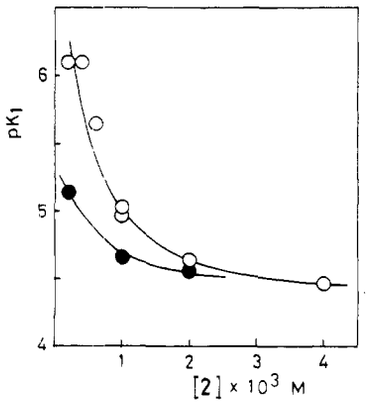

Figure 1. pK_1 of **2** as a function of concentration (25 °C): (○) the chloride of **2** without added salt; (●) with additional NaCl of 0.1 M.

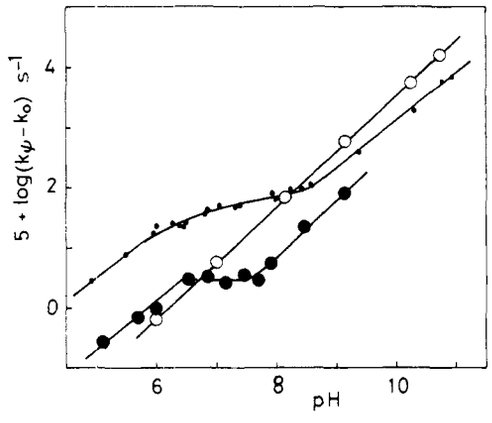

Figure 2. pH–rate profiles for the hydrolysis of phenyl acetates (**5**, n = 1): (○) **1a** = 1×10^{-4} M, substrate (X = p-NO_2) = 5×10^{-5} M; (•) **2** = 1×10^{-4} M, substrate (X = p-NO_2) = 5×10^{-5} M; (●) **2** = 2×10^{-3} M, substrate (X = p-OCH_3) = 2×10^{-4} M; obtained at 25 °C with 0.05 M buffer [acetate (pH < 6), phosphate (6 < pH < 7–8), Tris (pH ≃ 8), carbonate (pH > 9)].

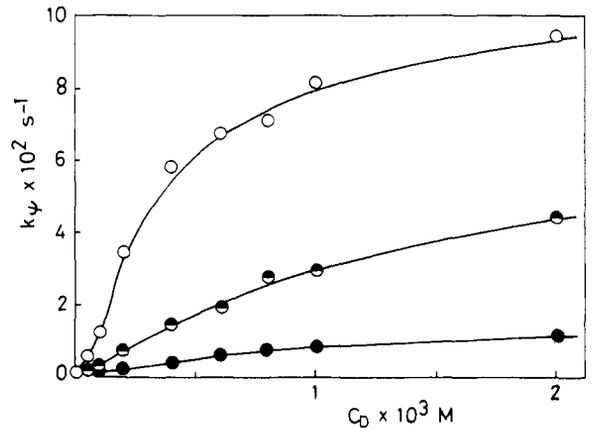

Figure 3. Plots of k_ψ vs. C_D of **2** at 25 °C and pH 8.07 (0.05M Tris buffer) (substrate = 5×10^{-5} M): (●) acetate (**5**; n = 1, X = p-NO_2); (◒) butyrate (**5**; n = 3, X = p-NO_2); (○) hexanoate (**5**, n = 5, X = p-NO_2).

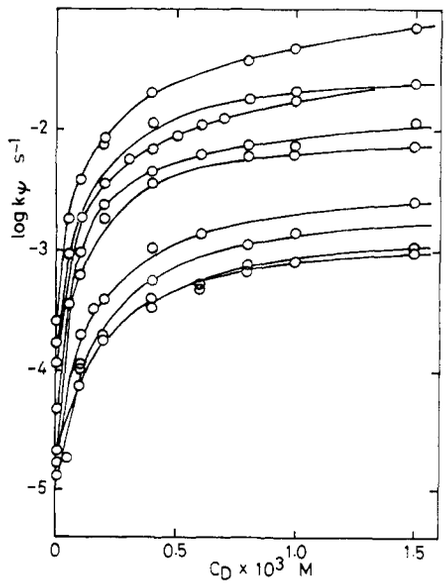

Figure 4. Substituent effects on the plots of k_ψ vs. C_D of **2** at 25 °C and pH 9.20 (0.05 M carbonate buffer); the curves from the top are for the acetates (**5**, n = 1) of X = p-NO_2, m-NO_2, p-$COCH_3$, p-t-Bu, p-CH_3, m-CH_3, H, and p-$COCH_3$ with the concentration = 2×10^{-4} M (except for p-NO_2 and p-$COCH_3$, 5×10^{-5} M).

by using eq 2–4: S, substrate; M, micelle; S–M, substrate–micelle complex; P, product; k_ψ, observed pseudo-first-order rate constant; k_o, spontaneous rate constant; k_m, catalytic rate constant; K_{app}, apparent association constant; C_D, surfactant monomer concentration; N, aggregation number. Any notable self-inhibition by the catalyst itself, often observed at higher C_D values,[17] was not detected in all of the present kinetics, which simplified the analyses. A problem may be the possible concentration dependency of pK_1 of **2** on C_D (Figure 1). Nevertheless, good linearity of eq 4 was obtained by assuming a constant pK_1 for each set of plots of k_ψ vs. C_D. Presumably, the presence of 0.05 M buffer sufficed for the constancy of pK_1 and cmc. Thus, the values of N/K_{app} and k_m could be readily obtained under various experimental conditions through the reciprocal plots of eq 4, where the cmc values were read from

Table II. Effects of Alkyl Chain Length of Substrate (5, X = *p*-NO_2) on the Rates of Micellar-Catalyzed Hydrolysis[a]

catalyst	pH[b]	*n*	$k_o \times 10^5$, s^{-1}	k_m, s^{-1}	N/K_{app}, mM	$k_m K_{app}/N$, $M^{-1}\,s^{-1}$	k_{rel}[c]
2	7.07	1[d]	0.216	0.035	2.98	11.7	
	7.14	5[e]	0.108	0.108	0.875	123	
	8.07	1	2.34	0.0455	3.85	11.8	172
		3[f]	1.65	0.0848	1.80	47.1	963
		5	0.955	0.125	0.669	187	5137
	9.20	1	32.5	0.450	9.13	49.3	
	9.47	3	23.8	1.00	2.76	362	
	9.20	5	20.0	1.25	0.832	1502	
1a	8.05	1	2.20	0.217	10.5	20.7	
		3	1.48	0.31	3.50	88.6	
		5	0.905	0.417	1.07	390	

[a] See Figures 3, 5, and 6. [b] 25 °C, 0.05 M buffer (see caption for Figure 2). [c] Relative to the rates of histamine (**3**); $(k_m K_{app}/N)/k_2$(histamine). [d] Registry no., 830-03-5. [e] Registry no., 956-75-2. [f] Registry no., 2635-84-9.

the plots of k_ψ vs. C_D (e.g., Figure 3) so as to obtain better fits of the data. Such cmc values varied within a range of 3–5 × 10^{-5} M. The aggregation number N has not been determined, so the N/K_{app} values are used in this paper to discuss binding phenomenon.

As mentioned above, the kinetic analyses of the related systems of **1b**,[9c] **1c**,[9d] and **4a**[8a] have been reported already. However, in the former two cases, attempts to measure K_{app} values failed to give reproducible results, so that only k_2' values were reported which were obtained from the slopes of the initial straight line portion of k_ψ vs. C_D plots. Meanwhile, substrate incorporation was examined in the mixed micelles of **4a**[8a] and **1b** with CTABr[9c] based on the kinetic scheme of eq 5–7. However, the K_i value was defined to be an inhibition constant due to the binding of substrate on an inactive region of micelle (M_i).[18] Here again the association constant K_{app} and the k_m values for the active micelle (M_a) and substrate remain inseparable from each other in the k_2 values.

$$S + M_i \overset{K_i}{\rightleftarrows} S\text{–}M_i \quad (5)$$

$$S + M_a \overset{k_2}{\rightarrow} X\text{–}M_a + P_1 \quad (6)$$

$$X\text{–}M_a + H_2O \overset{k_3}{\rightarrow} M_a + P_2 \quad (7)$$

Effect of Acyl Chain Length. The results of analyses of Figure 3 together with those for other pH values are shown in Table II. The apparent second-order rate constants k_2' (the initial slope of k_ψ vs. C_D plots) agreed well with the $k_m K_{app}/N$ values. These $k_m K_{app}/N$ values at pH 7–8 (plateau rates, Figure 2) may be compared with the reported k_2 values of **4a**:[8a] k_2 ($M^{-1}\,s^{-1}$, 25 °C) = 6.26 (n = 1), 22.5 (n = 3), and 122 (n = 5), respectively. It may be seen that **2** is roughly twice more reactive than **4a**. The k_{rel} values of Table II are also much larger than those of **4a** (relative to *N*-acetylhistidine). It should be noted that such a higher reactivity of **2** is achieved inspite of a lower pK_1 (~5) than that of **4a** (pK_1 = 6.2).[19]

The k_m values are roughly constant between pH 7–8 and increase at above pH 8, as expected for the undissociated neutral imidazole in the former and for the dissociated imidazole anion in the latter pH regions. The k_m value appears to be larger for a longer acyl chain substrate. This observation might be strange because the k_m values reflect the reactivities of substrates at the active site after their incorporation into the micelle, and they might be smaller for a longer acyl chain due to the unfavorable steric and electronic effects (see k_o values, later discussions, and Figure 8). The N/K_{app} values are independent of pH for n = 5 and slightly dependent for n = 1 and 3. The free energy change for the binding of substrate

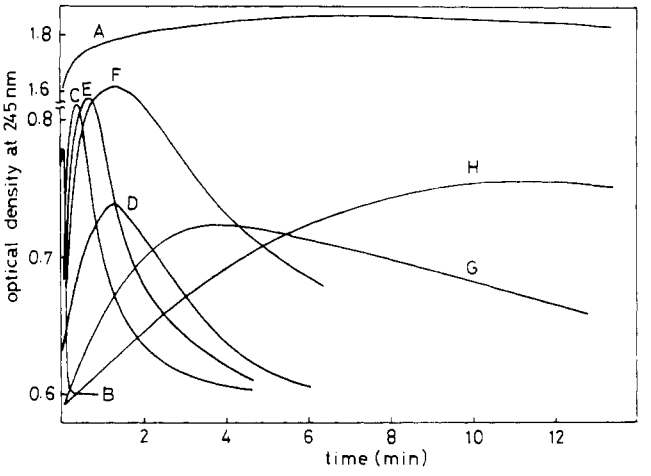

Figure 5. Spectrophotometric traces of the formation and decomposition of the acylimidazole intermediate in the hydrolysis of PNPA (**5**; n = 1, X = *p*-NO_2) = 1.58 × 10^{-4} M with the catalysts, [Im] = 5 × 10^{-3} M, in 0.05 M phosphate buffer at 25 °C: (A) **4b** (pH 8); (B) **1a** (9); (C) **1a** (8); (D) **1a** (7); (E) **2** (8); (F) **2** (7); (G) unsubstituted imidazole (8); (H) unsubstituted imidazole (7).

per methylene unit based on eq 8[8a] was calculated to be $-\Delta(\Delta F)$ = 260 (pH 8.07) and 355 (pH 9.20) cal mol^{-1} (25 °C), respectively, as approximate values. These values may be significantly smaller than the values of 630 cal mol^{-1} obtained from the K_i values of **4a**,[8a] and they might be related to a different mode of binding for the *p*-NO_2 ester (see later discussion).

$$\Delta(\Delta F) = \frac{-RT \ln (K_{app}/N)}{n} \quad (8)$$

In Table II are also listed the data for the catalysis of **1a**. They indicated several fold larger k_m and slightly larger N/K_{app} values as compared to those of **2**. However, as mentioned above, these data at pH 8 seem to be largely due to the activity of dissociated imidazole anion, so they cannot be directly compared with those of the neutral form of **2**.

Acylimidazole Intermediate. Previous studies have already demonstrated the intermediacy of acylimidazole for all **1a**,[9a] **1b**,[9c] **1c**,[9c-f] **4a**,[8a] and **4b**[9a] systems. The catalysis of **2** has also been observed to involve the acylimidazole intermediate as shown by the spectrophotometric traces at 245 nm in Figure 5. The figure indicates that the acylation of **4b** (OD increase) is fast, but its deacylation is very slow at pH 7. On the other hand, both steps are fast in the cases of **1a** and **2**. It is also indicated that the acylation rate in **2** is less sensitive to the change of pH (between 7–8) than in **1a**, in accord with the

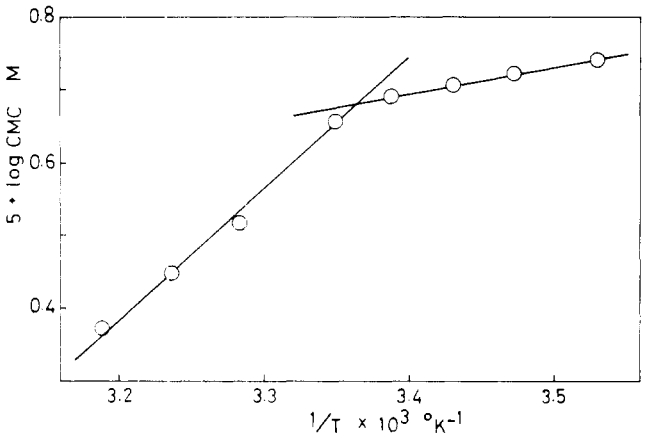

Figure 9. Plots of log cmc vs. $1/T$ (eq 12). The cmc values were observed at pH 9.30 (0.05 M carbonate buffer) with eosine = 1×10^{-5} M and **2** = 2×10^{-6}–1×10^{-4} M.

Table IV. Thermodynamic Parameters for the Micellization of 2[a]

temp range,[b] °C	$\Delta H°_m/(1+\alpha)$, kcal mol^{-1}	$\Delta S°_m/(1+\alpha)$, cal mol^{-1} deg^{-1}
10–23.9	1.70	33.5
23.9–40.6	8.29	55.7

[a] Calculated from the plots of Figure 9. [b] Other conditions: pH 9.3; 0.05 M carbonate buffer.

erature survey reveals that such a break is often observed for the electrolyte surfactants.[13,34]

Based on the phase separation model, Molyneux et al. have given eq 11 and 12 for the dilute aqueous solutions of elec-

$$\Delta G°_m = \Delta H°_m - T\Delta S°_m \quad (11)$$

$$\log C_f = \left[\frac{\Delta H°_m}{2.303R(1+\alpha)} \times \frac{1}{T}\right] - \frac{\Delta S°_m}{2.303R(1+\alpha)} + \log \omega \quad (12)$$

trolyte surfactants,[34c] where $\Delta G°_m$, $\Delta H°_m$, and $\Delta S°_m$ are the standard free energy change (kcal mol^{-1}) of micellization for the transfer of a mol of free monomer and α mol of the gegenion to the micellar phase and the corresponding standard enthalpy and entropy changes, respectively. C_f and ω are the molar concentrations of surfactant (i.e., cmc) and water (55.4 M, 20 °C), respectively. Thus, if the α values are known, the plots of Figure 9 allow the calculation of the $\Delta H°_m$ and $\Delta S°_m$ values from the slopes and intercepts. Unfortunately, the α values are unknown yet.[35] Nevertheless, it may be worthy to give $\Delta H°_m/(1+\alpha)$, $\Delta S°_m/(1+\alpha)$, and $\Delta G°_m/(1+\alpha)$ values as the qualitative measure of the thermodynamics of micellization of **2** as shown in Table IV.

In the literature, the micellization of nonionic surfactant was reported to give positive values of ΔH (~5 kcal mol^{-1}) and ΔS (~30 cal mol^{-1} deg^{-1}).[34e] On the other hand, some *N*-alkylbetaines were reported to give a negative ΔH at higher temperature and a positive ΔH at lower temperature, resulting in temperature minima in the plots of log cmc vs. $1/T$.[34d] The results in Figure 9 and Table IV resemble more the former case than the latter. Presumably, the hydrogen bonding between a water–imidazole unit in **2** and a water–oxymethylene unit in a nonionic surfactant may be more important in the monomer state than in the micellar aggregates. Such hydrogen bonding should be relatively unimportant for a betaine group. Loss of hydrogen bonding (liberation of water molecules) on micellization would result in positive values of both ΔH and ΔS as considered for hydrophobic bonding.[36] Liberation of solvated water from the imidazole group may partly contribute to the enhanced nucleophilicity of the imidazole group of **2** in addition to the electrostatic positive charge effect as suggested in the structure **9**. The smaller pK_1 of micellar **2** (~5) than that of nonmicellar reference histamine (**3**, 5.78) may also reflect the less polar nature of the micellar medium than that of bulk water.

Temperature Effects on the Rates. As discussed for the data in Figure 6, the rate-limiting step (measured by k_m) is likely to be different between σ and σ_p^- dependent esters. Namely, the addition of imidazole to the ester carbonyl (k_1 step in eq 9) is rate limiting for a σ dependent ester such as X = *p*-CH_3 (**5**), while the collapse of the tetrahedral intermediate (k_2 step) is rate limiting for a σ_p^- dependent ester such as X = *p*-NO_2. If such happens, the observed association constants K_{app}/N should also correspond to different equilibria, i.e., K for σ and $K(k_1/k_{-1})$ for σ_p^- dependent esters. Therefore, it is interesting to see the thermodynamic parameters for the two types of esters with respect to both k_m and K_{app}/N values.

p-Methyl- and *p*-nitrophenyl hexanoates (**5**, $n = 5$) were selected as the two extremes. They gave good reciprocal plots of eq 4 for various temperatures. The resulting K_{app}/N and k_m values were treated based on eq 13–16,[37] and the plots of log (K_{app}/N) and log (kT/hk_m) vs. $1/T$ allowed the calculation of the desired thermodynamic parameters, as shown in Figures 10 and 11 and Table V.

$$\Delta G = -2.303RT \log (K_{app}/N) \quad (13)$$

$$\Delta G = \Delta H - T\Delta S \quad (14)$$

$$\Delta G^{\ddagger} = -2.303RT \log (kT/hk_m) \quad (15)$$

$$\Delta G^{\ddagger} = \Delta H^{\ddagger} - T\Delta S^{\ddagger} \quad (16)$$

The activation parameters ($\Delta G^{\ddagger}$, $\Delta H^{\ddagger}$, and $\Delta S^{\ddagger}$) in Table V are the values for an intramolecular process. In this regard, it may be of interest to note that the $\Delta S^{\ddagger}$ values (−16.9 and −13.7 cal mol^{-1} deg^{-1}) are negatively much smaller than those of the following examples: −48.3 (*p*-CH_3) and −35.9 (*p*-NO_2) for a bimolecular nucleophilic catalysis of imidazole in the hydrolysis of phenyl acetates;[27] −50 to −60 for an intramolecular process of imidazole-containing polymer catalysts.[31a] However, it may be difficult to consider $\Delta H^{\ddagger}$ and $\Delta S^{\ddagger}$ separately because of their known compensatory relationship. In fact, the $\Delta H^{\ddagger}$ values of Table V are much larger than those of the reference examples (5–8 kcal mol^{-1}).[27,31a] At any rate, the $\Delta G^{\ddagger}$ values (20.5 and 17.6 kcal mol^{-1}) appear to be significantly smaller than expected for the values of an imidazole having such a low pK_a (~5). Another more striking feature in Table V are the parameters for the binding process (K_{app}/N) as discussed below.

In the case of the *p*-CH_3 ester, the data points in Figure 10 appear to be grouped in the two separate lines. They are scattered and the slopes of the lines are small, so that the calculated parameters in Table V inevitably involve considerable error and should be taken as approximate values. Nevertheless, it is certain that (1) the slopes of the two lines are both negative to give positive ΔH and ΔS values and (2) there is a break between the two lines near 297.1 K, which is mentioned above as a breaking temperature in the micellization of **2** (Figure 9). Thus, the two sets of positive ΔH and ΔS values for the *p*-CH_3 ester seem to be associated with a similar binding process as in micellization; namely, the ester is incorporated into the micelle by hydrophobic forces without involving any covalent bonding. These values are also similar, in both magnitude and sign, to those observed in the related

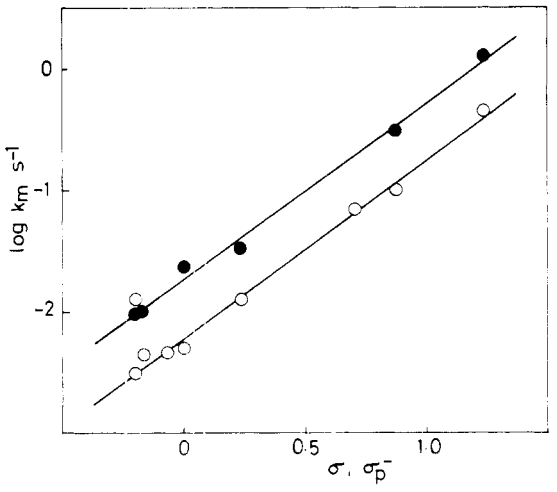

Figure 6. Plots of log k_m vs. σ and σ_p^- constants (see Table III): (○) acetates (**5**, n = 1); (●) hexanoates (**5**, n = 5).

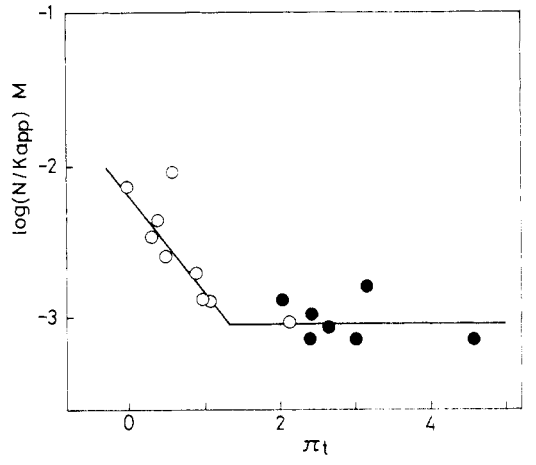

Figure 7. Plots of log (N/K_{app}) vs. π_t constants (see Table III): (○) acetates (**5**, n = 1); (●) hexanoates (**5**, n = 5).

dicated that the chymotrypsin-catalyzed hydrolysis of a nonspecific substrate such as p-nitrophenyl acetate proceeds through the acylation of an imidazole group at the active site of histidine.[29] A large positive ρ value for the σ_p^- correlation was then explained to indicate an extensive rupture of the C–O bond of the leaving group in the transition state for the imidazole acylation.[30] Thus, the present micellar catalysis resembles more the enzyme catalysis of chymotrypsin than the other nonmicellar model systems as far as concerning the substituent effect.

The above observations, i.e., the formation of acylimidazole and the log k_m^X vs. σ_p^- correlation, can be formulated in eq 9 by assuming a tetrahedral addition intermediate (**9**). En-

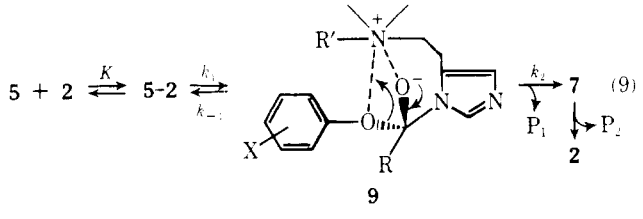

9

hanced nucleophilic reactivity of the micellar imidazole group would make a change in the rate-limiting step from k_1 (see **6**) to step k_2 for the esters substituted with a strong electron-withdrawing group. Development of a negative charge on the leaving phenoxide in the transition state would be far advanced in **9** due to a strong electrostatic interaction with the positive charge of the ammonium group in **9** to give σ_p^- dependency. Rate-limiting collapse of **9** may also account for a significant descrepancy between the pK_1 values determined by titration (~5) and observed in the pH–rate profile (~6). As noted in the effect of acyl chain length (Table II), the two parallel lines of Figure 6 again indicate more clearly that the longer chain hexanoates are always more reactive than the shorter chain acetates (except for p-t-Bu) in the micellar phase of **2**, in contrast with their reversed reactivities both in the bulk water and even in a nonfunctional micellar phase (Figure 8). Electronic and steric effects of the acyl chain on the nucleophilic attack of imidazole seem to be rather more unfavorable for hexanoates than for the acetates. Presumably, in the catalysis of **2** tighter binding, as manifested in the smaller N/K_{app} values, results in more lowering of the transition state energy.[31] Tighter binding would also increase such electrostatic interactions as depicted in **9** (see below for further discussion on the free energy change).

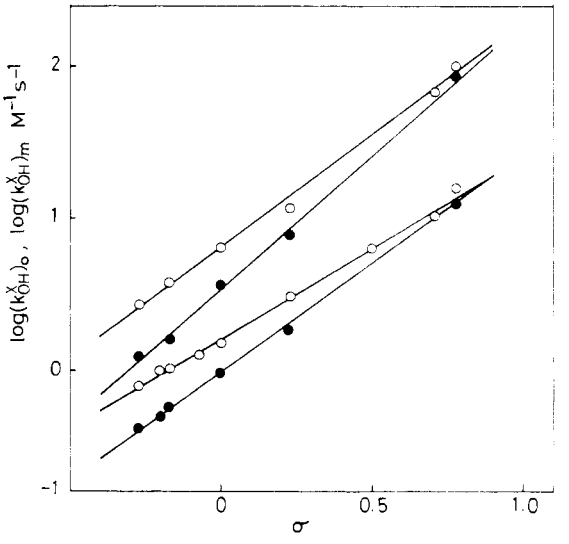

Figure 8. Plots of log $(k^X_{OH})_o$ and log $(k^X_{OH})_m$ vs. Hammett σ constants. $(k^X_{OH})_o$ and $(k^X_{OH})_m$ are the rate constants $k_\psi/[OH^-]$ in the absence (lower two lines) and presence (upper two lines) of STABr micelle ($C_D = 2 \times 10^{-3}$ M) with 0.05 M buffer ([OH^-] was calculated from the relation pOH$^-$ = 14 − pH): (○) acetates (**5**, n = 1); (●) hexanoates (**5**, n = 5).

The log (N/K_{app}) values appear to be better correlated with the π constants (a measure of hydrophobic effect)[32] rather than the σ constants (a measure of electronic effect). The plots of log (N/K_{app}) vs. σ gave only very scattered points. On the other hand, as shown in Figure 7 the plots with π_t values (eq 10)[33] indicate a definite trend of better binding for stronger

$$\pi_t = \pi_R + \pi_X \quad (10)$$

hydrophobic substrates, although the points are somewhat scattered. The figure also indicates a leveling off of binding; i.e., strong hydrophobic n-pentyl and $tert$-butyl groups overweigh the effects of other X substituents. Presumably, the point of log k_m for p-t-Bu (n = 1) in Figure 6 which deviates far from the n = 1 line is better grouped in with the points of the n = 5 line.

Temperature Effects on the Micellization of 2. In order to examine the temperature effect on the catalysis, it may also be necessary to know the temperature effects on the micellization itself. As shown in Figure 9, a sharp temperature break was observed in the plots of log cmc vs. $1/T$ at 297.1 K. A lit-

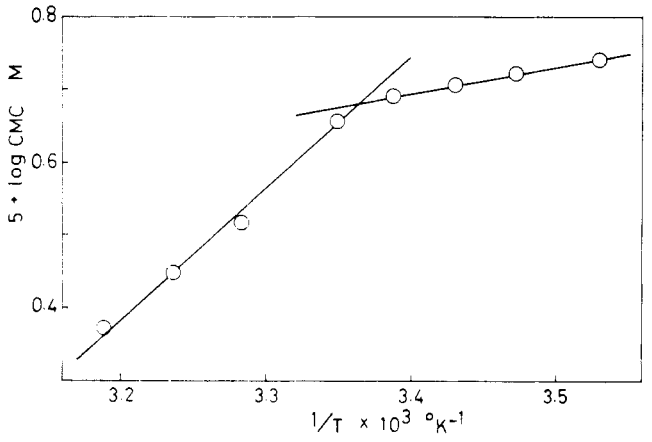

Figure 9. Plots of log cmc vs. $1/T$ (eq 12). The cmc values were observed at pH 9.30 (0.05 M carbonate buffer) with eosine = 1×10^{-5} M and **2** = 2×10^{-6}–1×10^{-4} M.

Table IV. Thermodynamic Parameters for the Micellization of 2[a]

temp range,[b] °C	$\Delta H°_m/(1+\alpha)$, kcal mol^{-1}	$\Delta S°_m/(1+\alpha)$, cal mol^{-1} deg^{-1}
10–23.9	1.70	33.5
23.9–40.6	8.29	55.7

[a] Calculated from the plots of Figure 9. [b] Other conditions: pH 9.3; 0.05 M carbonate buffer.

erature survey reveals that such a break is often observed for the electrolyte surfactants.[13,34]

Based on the phase separation model, Molyneux et al. have given eq 11 and 12 for the dilute aqueous solutions of elec-

$$\Delta G°_m = \Delta H°_m - T\Delta S°_m \quad (11)$$

$$\log C_f = \left[\frac{\Delta H°_m}{2.303R(1+\alpha)} \times \frac{1}{T}\right] - \frac{\Delta S°_m}{2.303R(1+\alpha)} + \log \omega \quad (12)$$

trolyte surfactants,[34c] where $\Delta G°_m$, $\Delta H°_m$, and $\Delta S°_m$ are the standard free energy change (kcal mol^{-1}) of micellization for the transfer of a mol of free monomer and α mol of the gegenion to the micellar phase and the corresponding standard enthalpy and entropy changes, respectively. C_f and ω are the molar concentrations of surfactant (i.e., cmc) and water (55.4 M, 20 °C), respectively. Thus, if the α values are known, the plots of Figure 9 allow the calculation of the $\Delta H°_m$ and $\Delta S°_m$ values from the slopes and intercepts. Unfortunately, the α values are unknown yet.[35] Nevertheless, it may be worthy to give $\Delta H°_m/(1+\alpha)$, $\Delta S°_m/(1+\alpha)$, and $\Delta G°_m/(1+\alpha)$ values as the qualitative measure of the thermodynamics of micellization of **2** as shown in Table IV.

In the literature, the micellization of nonionic surfactant was reported to give positive values of ΔH (~5 kcal mol^{-1}) and ΔS (~30 cal mol^{-1} deg^{-1}).[34e] On the other hand, some *N*-alkylbetaines were reported to give a negative ΔH at higher temperature and a positive ΔH at lower temperature, resulting in temperature minima in the plots of log cmc vs. $1/T$.[34d] The results in Figure 9 and Table IV resemble more the former case than the latter. Presumably, the hydrogen bonding between a water–imidazole unit in **2** and a water–oxymethylene unit in a nonionic surfactant may be more important in the monomer state than in the micellar aggregates. Such hydrogen bonding should be relatively unimportant for a betaine group. Loss of hydrogen bonding (liberation of water molecules) on micellization would result in positive values of both ΔH and ΔS as considered for hydrophobic bonding.[36] Liberation of solvated water from the imidazole group may partly contribute to the enhanced nucleophilicity of the imidazole group of **2** in addition to the electrostatic positive charge effect as suggested in the structure **9**. The smaller pK_1 of micellar **2** (~5) than that of nonmicellar reference histamine (**3**, 5.78) may also reflect the less polar nature of the micellar medium than that of bulk water.

Temperature Effects on the Rates. As discussed for the data in Figure 6, the rate-limiting step (measured by k_m) is likely to be different between σ and σ_p^- dependent esters. Namely, the addition of imidazole to the ester carbonyl (k_1 step in eq 9) is rate limiting for a σ dependent ester such as X = *p*-CH_3 (**5**), while the collapse of the tetrahedral intermediate (k_2 step) is rate limiting for a σ_p^- dependent ester such as X = *p*-NO_2. If such happens, the observed association constants K_{app}/N should also correspond to different equilibria, i.e., K for σ and $K(k_1/k_{-1})$ for σ_p^- dependent esters. Therefore, it is interesting to see the thermodynamic parameters for the two types of esters with respect to both k_m and K_{app}/N values.

p-Methyl- and *p*-nitrophenyl hexanoates (**5**, $n = 5$) were selected as the two extremes. They gave good reciprocal plots of eq 4 for various temperatures. The resulting K_{app}/N and k_m values were treated based on eq 13–16,[37] and the plots of log (K_{app}/N) and log (kT/hk_m) vs. $1/T$ allowed the calculation of the desired thermodynamic parameters, as shown in Figures 10 and 11 and Table V.

$$\Delta G = -2.303RT \log (K_{app}/N) \quad (13)$$

$$\Delta G = \Delta H - T\Delta S \quad (14)$$

$$\Delta G^{\ddagger} = -2.303RT \log (kT/hk_m) \quad (15)$$

$$\Delta G^{\ddagger} = \Delta H^{\ddagger} - T\Delta S^{\ddagger} \quad (16)$$

The activation parameters ($\Delta G^{\ddagger}$, $\Delta H^{\ddagger}$, and $\Delta S^{\ddagger}$) in Table V are the values for an intramolecular process. In this regard, it may be of interest to note that the $\Delta S^{\ddagger}$ values (−16.9 and −13.7 cal mol^{-1} deg^{-1}) are negatively much smaller than those of the following examples: −48.3 (*p*-CH_3) and −35.9 (*p*-NO_2) for a bimolecular nucleophilic catalysis of imidazole in the hydrolysis of phenyl acetates;[27] −50 to −60 for an intramolecular process of imidazole-containing polymer catalysts.[31a] However, it may be difficult to consider $\Delta H^{\ddagger}$ and $\Delta S^{\ddagger}$ separately because of their known compensatory relationship. In fact, the $\Delta H^{\ddagger}$ values of Table V are much larger than those of the reference examples (5–8 kcal mol^{-1}).[27,31a] At any rate, the $\Delta G^{\ddagger}$ values (20.5 and 17.6 kcal mol^{-1}) appear to be significantly smaller than expected for the values of an imidazole having such a low pK_a (~5). Another more striking feature in Table V are the parameters for the binding process (K_{app}/N) as discussed below.

In the case of the *p*-CH_3 ester, the data points in Figure 10 appear to be grouped in the two separate lines. They are scattered and the slopes of the lines are small, so that the calculated parameters in Table V inevitably involve considerable error and should be taken as approximate values. Nevertheless, it is certain that (1) the slopes of the two lines are both negative to give positive ΔH and ΔS values and (2) there is a break between the two lines near 297.1 K, which is mentioned above as a breaking temperature in the micellization of **2** (Figure 9). Thus, the two sets of positive ΔH and ΔS values for the *p*-CH_3 ester seem to be associated with a similar binding process as in micellization; namely, the ester is incorporated into the micelle by hydrophobic forces without involving any covalent bonding. These values are also similar, in both magnitude and sign, to those observed in the related

Table V. Thermodynamic Parameters for the Hydrolysis of Hexanoate 5 Catalyzed by Micellar 2[a]

	k_m			K_{app}/N			
X	$\Delta G^{\ddagger}$,[b] kcal mol^{-1}	$\Delta H^{\ddagger}$, kcal mol^{-1}	$\Delta S^{\ddagger}$, cal mol^{-1} deg^{-1}	ΔG,[b] kcal mol^{-1}	ΔH, kcal mol^{-1}	ΔS, cal mol^{-1} deg^{-1}	temp range, °C
p-CH_3	20.5	15.4	−16.9	−4.66	3.63	27.8	14.9–22
				−4.75	1.60	21.3	25–39
p-NO_2	17.6	13.5	−13.7	−4.62	−11.9	−24.5	10.5–30

[a] Calculated from the plots of Figures 10 and 11. [b] For the values at 298.2 K.

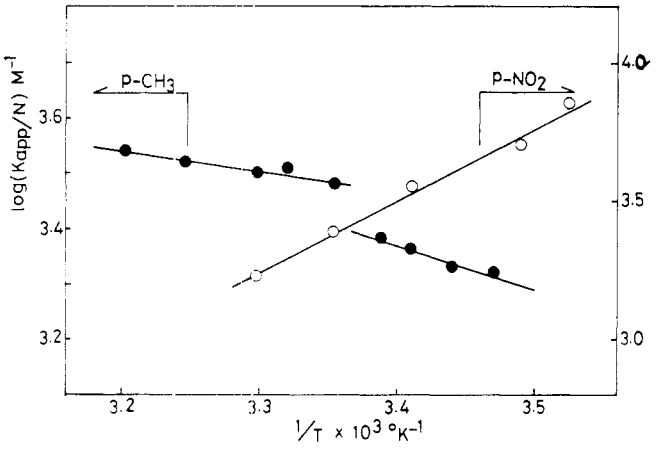

Figure 10. Plots of log (K_{app}/N) vs. $1/T$ (eq 13 and 14). The K_{app}/N values were obtained from the plots of eq 4 for the catalysis of **2** at pH 9.2 (0.05 M carbonate buffer) and at the following temperatures: for p-methylphenyl hexanoate (**5**, n = 5, X = p-CH_3; 2×10^{-4} M), 14.9, 17.4, 20.1, 22.0, 25.0, 28.0, 30.0, 35.0, and 39.0 °C; and for p-nitrophenyl hexanoate (**5**, n = 5, X = p-NO_2; 5×10^{-5} M), 10.5, 13.1, 20.0, 25.0, and 30.0 °C.

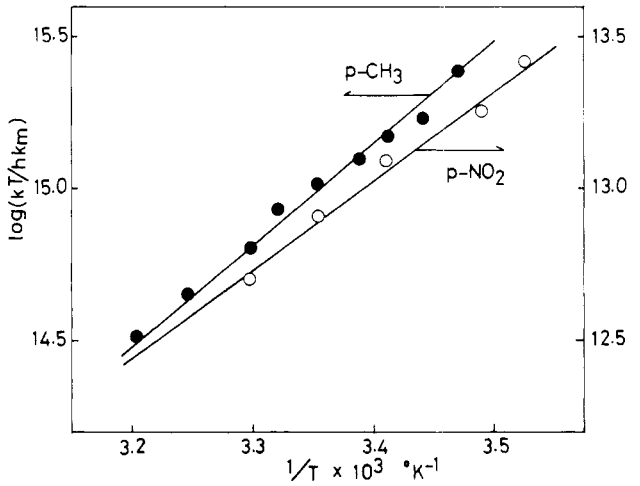

Figure 11. Plots of log (kT/hk_m) vs. $1/T$ (eq 15 and 16); see Figure 10.

polymer catalysis.[31a] On the other hand, the data points of the p-NO_2 ester in Figure 10 give a single straight line and the slope is positive to give negative ΔH and ΔS values. These large negative enthalpy and entropy changes appear to be difficult to account for by any electrostatic or hydrogen bonding, as well as hydrophobic, interactions as long as a noncovalent binding process is concerned. As presumed above, this difficulty may be solved by including the tetrahedral intermediate (**9**, eq 9) in the preequilibrium binding process; the stabilization of the intermediate by electrostatic interaction should give favorable enthalpy and unfavorable entropy changes.

Concluding Remarks. It is well known that a simple mixture of cationic micelle and a hydrophilic imidazole derivative does not create any micellar activation, but rather causes an inhibition of the imidazole function because of their partition into different phases.[1,8a] While a combination of a cationic micelle and an imidazole derivative which can be incorporated into the micellar phase yields a remarkable activation of imidazole nucleophilicity. Such activation does not necessarily require 1:1 ion pair formation as in **4** because a neutral hydrophobic imidazole can also be activated in a cationic micelle.[12] Presumably, the dipolar aprotic nature of the micellar medium is responsible for such activation of nucleophile. An interesting possibility is a cooperative electrophilic catalysis by the micellar positive charge in such a manner as to stabilize the transition state. However, it may not be easy to prove such a catalysis in the systems of mixed micelles so far examined. An important conclusion of the present study is the reality of such catalysis to occur as depicted in the structures **6**, **7**, and **9**. This conclusion appears to have been reached by successful separation of k_m and K_{app}/N values.

Experimental Section

Materials. Water for kinetics and analysis was obtained by distilling deionized water twice. Buffer reagents (CH_3COOH, CH_3COONa, Na_2HPO_4, KH_2PO_4, $NaHCO_3$, Na_2CO_3, $(HOCH_2)_3CNH_2$, NaOH, hydrochloric acid, etc.), eosine yellow ($C_{20}H_6Br_4Na_2$), histamine dihydrochloride, and other reagents for analysis were commercial extra pure reagents. Acetonitrile for the stock solution of ester substrates was refluxed on phosphorus pentoxide and carefully distilled. Octadecylamine and octadecylbromide were IR- and GLC-pure commercial reagents and were further purified if necessary. Dimethyloctadecylamine was prepared by reacting octadecylamine with formaldehyde and formic acid, bp 168 ° (3 mmHg).[38] Octadecyltrimethylammonium bromide (STABr) was prepared by reacting octadecyl bromide with trimethylamine in ethanol and was purified by precipitation and recrystallization. Hexadecyltrimethylammonium bromide (CTABr) was a commercial reagent. *N*-Myristoylhistidine was prepared according to the literature method.[8a] 4-(Hydroxymethyl)imidazole hydrochloride (mp 108 °C),[39] 4-(chloromethyl)imidazole hydrochloride (mp 142 °C),[40] and 4-(2-chloroethyl)imidazole hydrochloride (mp125–126 °C)[41] were prepared and purified according to literature procedures. Substituted phenyl carboxylates were prepared by reacting the corresponding substituted phenols with acyl chlorides in mixed pyridine–benzene and were purified by distillation or recrystallization (methanol or ligroin) according to literature procedures; their properties are listed in Table VI.

Dimethyl[(4-imidazolyl)methyl]octadecylammonium Chloride (1a) Hydrochloride. 4-(Chloromethyl)imidazole (5.7 g) and dimethyloctadecylamine (22.5 g) were dissolved in 100 mL of anhydrous ethanol and reacted in an autoclave at 80 °C for 2 days. Into the reaction mixture was introduced dry ammonia gas under ice cooling, and the resulting solid ammonium chloride was removed by filtration. The filtrate was concentrated, and ether was added to the residue to give a precipitate. The precipitate was further treated with ethanol–ether in order to remove excess dimethyloctadecylamine and finally with HCl in ethanol to convert the free imidazole to its hydrochloride. Ethanol was removed, and the residue was carefully recrystallized from ethanol–ether to give an amorphous powder (ca. 20% yield) which melted at 65–68 °C by forming liquid crystals which decomposed at 178 °C: NMR (60 MHz) τ (D_2O) 2.2 (1 H, s), 2.46 (1

Table VI. List of Ester Substrates (5)

5	X	bp, °C (mmHg)	mp, °C	λ_{max}, nm[a]
acetates (n = 1)	p-NO_2		77–78	400
	m-NO_2		55–56	405
	p-$COCH_3$		51.5–53	327
	p-Cl	113 (18)		303
	H	87 (20)		270
	p-CH_3	123–124 (15)		279
	m-CH_3	97–98 (18)		279
	p-OCH_3	131 (21)	31–32	289
	p-t-Bu	128–128.5 (18)		278
butyrate (n = 3)	p-NO_2	122–124 (1.5)		400
hexanoates (n = 5)	p-NO_2	137–139 (1.0)		400
	p-$COCH_3$	194–195.5 (17)		327
	p-Cl	101–102 (1.0)		303
	H	92–93 (1.0)		270
	p-CH_3	96–97 (1.0)		279
	p-t-Bu	136–139 (2.0)		278
	p-OCH_3	120 (1.0)		289

[a] Absorption wavelength of phenols used for kinetics (pH 9.2 under micellar conditions).

H, s), 5.56 (2 H, N^+CH_2Im), 6.7 (br, ca. 2 H), 6.9 (ca. 6 H, s), 8.62 (br, ca. 32 H), 9.03 (3 H, t). Anal. Calcd for $C_{24}H_{49}Cl_2N_3$: C, 63.96; H, 10.98; Cl, 15.73; N, 9.33. Found: C, 63.82; H, 11.30; Cl, 5.95; N, 9.13.

Dimethyl[2-(4-imidazolyl)ethyl]octadecylammonium Chloride (2) Hydrochloride. 4-(2-Chloroethyl)imidazole hydrochloride (10 g, 0.06 mol) was dissolved in 30 mL of anhydrous ethanol, and to this was added 22.5 mL of 3 N ammonia in ethanol under ice cooling. The resulting ammonium chloride was filtered off, and dimethyloctadecylamine (35.6 g, 0.12 mol) was added to the filtrate. This reaction mixture was refluxed for 92 h, treated again with ammonia–ethanol, concentrated to 100 mL, diluted with 400 mL of ether, and finally left for precipitation under cooling. The precipitate was treated with charcoal in hot acetonitrile and recrystallized to give 11.3 g (44%) of colorless crystalline powder. Additionally, about a 60% total yield was obtained. This product was further treated with HCl in ethanol and carefully recrystallized with ethanol–ether to give the desired pure hydrochloride: mp 85–86 °C, decomposed at 152 °C; NMR (60 MHz) τ (D_2O) 2.2 (1 H, s), 2.9 (1 H, s), 6.3–7.2 (br, ca. 4 H), 6.83 (ca. 6 H, s), 8.72 (br, ca. 32 H), 9.13 (3 H, t). Anal. Calcd for $C_{25}H_{51}Cl_2N_3$: C, 62.12; H, 10.22; N, 8.95. Found: C, 62.20; H, 10.69; N, 8.90.

pH Measurements. A Hitachi-Horiba pH meter/F-7DE was used and standardized using certified standard buffers: pH 6.86 (25 °C, JIS-Z880a, phosphate buffer) and 9.12 (25 °C, JIS-A8002, borate buffer). The glass electrode was carefully rinsed with pure water before and after each measurement. The pH of the reaction mixture was measured before and after the reaction, and when these two pH readings differed by more than ±0.04 unit the run was discarded.

p*K* Determinations. In a thermostated water bath (25 °C), an acidified solution of **2** (pH 3–4, with HCl) was titrated with a concentrated sodium hydroxide solution with stirring by using a microburet and an above pH meter. The data were treated by the modified Henderson equation,[15] and the results are shown in Figure 1.

Cmc Determination.[14] Solutions of varied concentrations of **2**, each containing 1×10^{-5} M of eosine, were made up with 0.05 M buffer of given pH. Absorbances of these solutions at 517 and 529 nm were measured spectrophotometrically in a thermostated cell by using a Hitachi 124 spectrophotometer. The plots of absorbance vs. surfactant concentration (C_D) always gave sharp breaks at the cmc for each wavelength under various conditions (pH and temperature, etc.).

Kinetic Measurements. The general procedure was the following. A 3-mL amount of reaction solution of given pH containing the catalyst of desired concentration, if any, was temperature equilibrated in a quartz cell placed in a Hitachi 124 spectrophotometer. To this solution was added 30 μL of ester solution in acetonitrile by using a small polyethylene rod having a pedestal for both holding the ester solution and mixing, and the absorbance of liberated phenol (see Table VI) was recorded. Rate constants were calculated using the absorbance at infinite time determined for each run and by using the integrated first-order equation $k_\psi = (2.03/t) \log [(OD_\infty - OD_t)/(OD_\infty - OD_0)]$.

Acknowledgment. This research was supported in part by a Grant-in-Aid for Scientific Research from the Ministry of Education, Japan.

Registry No.—**1a** HCl, 68437-50-3; **2** HCl, 68437-51-4; **4b**, 68538-74-9; 4-(chloromethyl)imidazole, 23785-22-0; dimethyloctadecylamine, 124-28-7; 4-(2-chloroethyl)imidazole hydrochloride, 27275-48-5.

References and Notes

(1) (a) E. H. Cordes and R. B. Dunlap, *Acc. Chem. Res.*, **2**, 329 (1969); (b) E. H. Cordes and C. Gitler, *Prog. Bioorg. Chem.*, **2**, 1 (1973); (c) E. H. Cordes, Ed., "Reaction Kinetics in Micelles", Plenum Press, New York, 1973; (d) J. H. Fendler and E. J. Fendler, "Catalysis in Micellar and Macromolecular Systems", Academic Press, New York, 1975; (e) C. A. Bunton, "Micellar Reactions" in "Application of Biochemical Systems in Organic Chemistry", Part 2, J. B. Jones, C. J. Sih, and D. Perlman, Eds., Wiley, New York, 1976, Chapter 4.
(2) (a) T. C. Bruice, J. Katzhendler, and L. R. Fedor, *J. Am. Chem. Soc.*, **90**, 1333 (1968); (b) C. A. Blyth and J. R. Knowles, *ibid.*, **93**, 3017 (1971); (c) D. G. Oakenfull, *J. Chem. Soc., Perkin Trans. 2*, 1006 (1973).
(3) (a) P. Heitmann, *Eur. J. Biochem.*, **5**, 305 (1968); (b) W. Tagaki, T. Amada, Y. Yamashita, and Y. Yano, *J. Chem. Soc., Chem. Commun.*, 1131 (1972).
(4) (a) G. Meyer, *Tetrahedron Lett.*, 4581 (1972); (b) G. Meyer, *C. R. Hebd. Seances Acad. Sci., Ser. C*, **276**, 1599 (1973); (c) M. Chevion, J. Katzhendler, and S. Sarel, *Isr. J. Chem.*, **10**, 795 (1972); (d) V. Gani, C. Lapinte, and P. Viout, *Tetrahedron Lett.*, 4435 (1973); (e) K. Martinek, A. V. Levashov, and I. V. Berezin, *Tetrahedron Lett.*, 1275 (1975); (f) R. A. Moss, R. C. Nahas, S. Ramaswami, and W. J. Sanders, *ibid.*, 3379 (1975); (g) A. K. Yatsimirski, K. Martinek, and I. V. Berezin, *Tetrahedron*, **27**, 2855 (1971).
(5) E. Zeffren and R. E. Watson, *Intra-Sci. Chem. Rep.*, **6**, 51 (1972).
(6) (a) C. A. Bunton, L. Robinson, and M. F. Stam, *Tetrahedron Lett.*, 121 (1971); (b) C. A. Bunton and L. G. Ionescu, *J. Am. Chem. Soc.*, **95**, 2912 (1973); (c) C. A. Bunton, L. Robinson, and M. Stam, *ibid.*, **92**, 7393 (1970); (d) C. A. Bunton and S. Diaz, *ibid.*, **98**, 5663 (1976).
(7) C. A. Blyth and J. R. Knowles, *J. Am. Chem. Soc.*, **93**, 3021 (1971).
(8) (a) C. Gitler and A. Ochoa-Solano, *J. Am. Chem. Soc.*, **90**, 5004 (1968); (b) T. E. Wagner, C. Hsu, and C. S. Pratt, *ibid.*, **89**, 6366 (1967); (c) P. Heitmann, R. Husung-Bublits, and H. J. Zunft, *Tetrahedron*, **30**, 4137 (1974).
(9) (a) W. Tagaki, M. Chigira, T. Amada, and Y. Yano, *J. Chem. Soc., Chem. Commun.*, 219 (1972); (b) W. Tagaki, S. Kobayashi, and D. Fukushima, *ibid.*, 29 (1977); (c) U. Tonellato, *J. Chem. Soc., Perkin Trans. 2*, 771 (1976); (d) *ibid.*, 821 (1977); (e) L. Anoardi and U. Tonellato, *J. Chem. Soc., Chem. Commun.*, 401 (1977); (f) R. A. Moss, R. C. Nahas, and S. Ramaswami, *J. Am. Chem. Soc.*, **99**, 627 (1977); (g) R. A. Moss, T. J. Lukas, and R. C. Nahas, *Tetrahedron Lett.*, 3851 (1977).
(10) (a) J. M. Brown and C. A. Bunton, *J. Chem. Soc., Chem. Commun.*, 960 (1974); (b) J. M. Brown, C. A. Bunton, and S. Diaz, *ibid.*, 971 (1974).
(11) J. P. Guthrie and Y. Ueda, *Can. J. Chem.*, **54**, 2745 (1976).
(12) (a) T. Kunitake, Y. Okahata, and T. Sakamoto, *Chem. Lett.*, 459 (1975); (b) Y. Okahata, R. Ando, and T. Kunitake, *J. Am. Chem. Soc.*, **99**, 3067 (1977).
(13) I. Tabushi and Y. Kuroda, *Tetrahedron Lett.*, 4435 (1973).
(14) M. L. Corrin and W. D. Harkins, *J. Am. Chem. Soc.*, **69**, 679 (1947).
(15) (a) A. Katchalsky and P. Spitnik, *J. Polym. Sci.*, **2**, 432 (1947); (b) A. Katchalsky, N. Shavit, and H. Eisenberg, *ibid.*, **13**, 69 (1954).
(16) (a) The analysis of Figure 2 based on $k_\psi = k_c K_{app}/(a_{H^+} + K_{app})$ failed to give a reliable pK_1 value. While, in another study on the micellar-catalyzed hydrolysis of triaryl phosphate by **2**, we have been able to observe such a kinetic pK_1 (5.3): W. Tagaki, T. Eiki, and H. Kaneko, 26th IUPAC Congress, Abstracts Session 1, 8F309, Tokyo, 1977, p 199. (b) Micellar-catalyzed hydrolysis of bis(4-nitrophenyl) sulfate indicated the kinetic pK_2 of **2** to be 13: T. Eiki and W. Tagaki, 37th Annual Meeting of the Japan Chemical Society, Abstracts 2, 1978, p 694.

(17) Another different scheme may also be applied, but was not examined here; see D. Piszkiewicz, *J. Am. Chem. Soc.*, **99**, 1550, 7695 (1977).
(18) Both N/K_{app} and K_i are apparent dissociation constants of the 1:1 complex of monomer surfactant and substrate.
(19) In the nonmicellar imidazole-catalyzed hydrolysis of *p*-nitrophenyl acetate (**5**; $n = 1$, X = *p*-NO_2), it was found that the rate of nucleophilic attack of imidazoles (k_N) was related to the pK_a values by the equation $\log k_N = 0.8pK_a - 4.30$. See T. C. Bruice and G. L. Schmir, *J. Am. Chem. Soc.*, **80**, 148 (1958).
(20) The same $\Delta pK = pK(\text{micelle}) - pK(\text{nonmicelle}) = -1.8$ was observed in 20% aqueous ethanol for the dissociation of 4-hexyl-2-nitrophenol for each **1a**, **2**, and STABr surfactant: T. Kitahara, Thesis, Gunma University, 1974.
(21) An idea has been advanced that a hydrophobic nucleophile produces a highly nucleophilic ion with a hydrophobic cation.[12b]
(22) A. Kurashima, Thesis, Gunma University, 1978; Y. Yano, Y. Yoshida, A. Kurashima, Y. Tamura, and W. Tagaki, *J. Chem. Soc., Perkin Trans. 2*, submitted for publication.
(23) J. F. Kirsch and W. P. Jencks, *J. Am. Chem. Soc.*, **86**, 837 (1964).
(24) (a) T. C. Bruice and S. J. Benkovic, "Bioorganic Mechanism", Vol. 1, W. A. Benjamin, New York, 1966; (b) W. P. Jencks, "Catalysis in Chemistry and Enzymology", McGraw-Hill, New York, 1969.
(25) C. D. Ritchie and W. F. Sager, *Prog. Phys. Org. Chem.*, **2**, 323 (1964).
(26) T. C. Bruice and S. J. Benkovic, *J. Am. Chem. Soc.*, **86**, 418 (1964).
(27) T. C. Bruice, *J. Am. Chem. Soc.*, **81**, 5444 (1959).
(28) M. L. Bender and K. Nakamura, *J. Am. Chem. Soc.*, **84**, 2577 (1962).
(29) C. D. Hubbard and J. F. Kirsch, *Biochemistry*, **11**, 2483 (1972).
(30) See also the discussion in W. P. Jencks and M. Gilchrist, *J. Am. Chem. Soc.*, **90**, 2622 (1968).
(31) In some related polymer catalyses, tight binding was found to lead to either (a) unfavorable or (b) favorable free energy of activation: (a) T. Kunitake and S. Shinkai, *J. Am. Chem. Soc.*, **93**, 4247, 4256 (1971); (b) *Makromol. Chem.*, **151**, 127 (1972).
(32) Review: (a) A. Leo, C. Hansch, and D. Elkins, *Chem. Rev.*, **71**, 525–616 (1971); (b) T. Fujita, J. Iwasa, and C. Hansch, *J. Am. Chem. Soc.*, **86**, 5175 (1964).
(33) The π_t values are taken arbitrarily as the measure of combined hydrophobicity of the two parts of the ester. The π_R and π_X values are calculated from Table XVII of ref 32a based on $\pi_{R(X)} = (\log P_{R(X)} - \log P_H)$ for RCO_2H (R = CH_3, C_5H_{11}, H) and the substituted phenoxyacetic acid, $XC_6H_4O\text{-}CH_2CO_2H$.
(34) (a) E. D. Goddard and G. C. Benson, *Can. J. Chem.*, **35**, 986 (1957); (b) E. D. Goddard, C. A. J. Hoeve, and G. C. Benson, *J. Phys. Chem.*, **61**, 593 (1957); (c) P. Molyneux, C. T. Rhodes, and J. Swarbrick, *Trans. Faraday Soc.*, **61**, 1043 (1965); (d) J. Swarbrick and J. Daruwala, *J. Phys. Chem.*, **73**, 2627 (1969); (e) M. J. Schick, *ibid.*, **67**, 1796 (1963); (f) M. F. Emerson and A. Holtzer, *ibid.*, **71**, 3320 (1967).
(35) At higher pH, the α value of **2** should approach 0 as in the cases of betaine-type surfactants due to the formation of imidazole anion. The values $\alpha = 0.37$ for alkyltrimethylammonium halide ($RNMe_3^+X^-$) and 0.56 for alkylammonium halide ($RNH_3^+X^-$) were reported.[34c]
(36) (a) W. Kauzmann, *Adv. Protein Chem.*, **14**, 1 (1959); (b) G. Nemethy and H. A. Scheraga, *J. Phys. Chem.*, **66**, 1773 (1962).
(37) A. A. Frost and R. G. Pearson, "Kinetics and Mechanism", 2nd ed., Wiley, New York, 1961, p 98.
(38) H. F. Clark, H. B. Gillespie, and S. Z. Weisshaus, *J. Am. Chem. Soc.*, **55**, 4571 (1933).
(39) E. C. Horning, "Organic Syntheses", Collect. Vol. 3, Wiley, New York, 1962, p 460.
(40) R. A. Turner, C. F. Huebner, and C. R. Scholz, *J. Am. Chem. Soc.*, **71**, 2801 (1949).
(41) C. F. Huebner, *J. Am. Chem. Soc.*, **73**, 4668 (1951).

Free-Radical Reactions of Fluoroalkanesulfenyl Halides. 3.[1a] Reactions of Fluoroalkane- and Chlorofluoroalkanesulfenyl Chlorides with Hydrocarbons

J. F. Harris, Jr.

Central Research and Development Department,[2] Experimental Station, E. I. du Pont de Nemours and Company, Wilmington, Delaware 19898

Received May 8, 1978

Free-radical reactions of several fluoroalkane- and chlorofluoroalkanesulfenyl chlorides with toluene, cyclohexane, and butane have been studied. The organic products obtained from these reactions include thiols, disulfides, sulfides, and chlorohydrocarbons. The relative yields of these products depend upon the structure of both the sulfenyl chloride and the hydrocarbon. Steric arguments are proposed to account for the results.

Following a long period of concentration upon the ionic reactions of sulfenyl halides,[3] recent years have seen the beginnings of interest in the free-radical chemistry of these materials. Free-radical additions to olefins have been demonstrated,[4,5] and reactions with hydrocarbons yielding disulfides, sulfides, and/or chlorohydrocarbons have also been reported.[1,6–10] In the previous paper of this series, free-radical chain reactions of CF_3SCl with several hydrocarbons containing alkane C–H bonds were found to yield trifluoromethyl hydrocarbyl sulfides, bis(trifluoromethyl) disulfide, and chlorohydrocarbons, the relative proportions depending upon the structure of the hydrocarbon.[1a] This paper presents the results of a study of the free-radical reactions of several fluoroalkane- and chlorofluoroalkanesulfenyl chlorides with hydrocarbons aimed at assessing the influence of the structure of the sulfenyl chloride upon the course of the reaction.

Results and Discussion

The sulfenyl chlorides studied were **1–6**. Photoinitiated reactions of each of these with excess cyclohexane, toluene, and *n*-butane were examined. The results of the reactions are tabulated in Tables I–III and are discussed below.

$(CF_3)_3CSCl$ $(CF_3)_2CFSCl$ $n\text{-}C_3F_7SCl$
1 **2** **3**

HCF_2CF_2SCl $ClCF_2SCl$ Cl_2CFSCl
4 **5** **6**

The reactions examined yielded four types of organic compounds as major products: thiols, disulfides, sulfides, and chlorohydrocarbons—one, two, or three of which may predominate in a particular reaction, depending upon the structure of the sulfenyl chloride and the hydrocarbon.

$$R_fSCl + RH \xrightarrow{h\nu} R_fSH + R_fSSR_f + R_fSR + RCl + HCl \quad (1)$$

In no case were all four obtained as major products.

The reactions of perfluoro-*tert*-butanesulfenyl chloride (**1**) as a group were unique in that the only major products detected were the thiol and the chlorohydrocarbon (eq 2). Thus from cyclohexane, perfluoro-*tert*-butanethiol (**7**) and chlorocyclohexane were obtained.

$$\underset{\mathbf{1}}{(CF_3)_3CSCl} + RH \xrightarrow{h\nu} \underset{\mathbf{7}}{(CF_3)_3CSH} + RCl \quad (2)$$

In all three cases at most traces of HCl were noted during the irradiation period, and one to several trace unknowns were detected by gas chromatography (GC). In the reaction with

0022-3263/79/1944-0563$01.00/0